

Description of nuclear properties for $^{114-128}\text{Cd}$ isotopes

A. Mohammed Ali^a, R. B. Alkhayat^a, M. M. Yousif^a, M. Abed Al-Jubbori^a, H. H. Kassim^b, and F. I. Sharrad^{b,c}

^aDepartment of Physics, College of Education for Pure Sciences, University of Mosul, 41001 Mosul, Iraq.

^bDepartment of Physics, College of Science, University of Kerbala, Iraq.

^cCollege of Health and Medical Technology, University of AlKafeel, Iraq.

Received 5 November 2021; accepted 22 April 2022

In this paper, the energy levels of the ground-state band (GSB) and other states for $^{114-128}\text{Cd}$ isotopes have been determined using the Interacting Boson Model (IBM-1) with a New Empirical Equation (NEE). The GSB results showed that the IBM-1, NEE, and available experimental data were all in fairly consistent. The NEE and IBM-1 calculations for the high states above 6^+ state are slightly overestimated compared to the experimental data, with the exception of the ^{114}Cd and ^{118}Cd nuclei. Furthermore, the reduced transition probabilities $B(E2)$ extracted from the IBM-1 model agree well with the available experimental data. The potential energy surface (EPS) was also examined with the IBM-1. The EPS contour results for Cd isotopes demonstrate that the Cd isotopes under investigation represent a smooth transition behavior from light Cd nuclei toward a more collective vibrational mode as the neutron number increases.

Keywords: IBM-1; energy level; potential energy; cadmium isotopes; NEE.

DOI: <https://doi.org/10.31349/RevMexFis.68.060401>

1. Introduction

The Cd isotopes are of specific interest since they have only two fewer protons than the individual closed-shell Sn nuclei. The large abundance of stable isotopes in combination with the interesting properties of the closed proton shell near $Z=50$ and the presence of neutrons in the middle of the $N=50-82$ shell make the $Z=50$ region favored for nuclear structure studies [1–4]. Schraff-Goldhaber and Wesener observed that The Cd isotopes have low lying states that reflect the quadrupole-vibrational excitations of a spherical-equilibrium surface [5]. Iachello and Arima [6] successfully described the collective nuclear properties in intermediate-mass nuclei using the Interacting Boson Model (IBM-1). Moreover, the IBM-1 model generated the $U(6)$ group algebra, that then produces three subgroup symmetries: $U(5)$, $SU(3)$, and $O(6)$. These three dynamics are associated with a vibrational, rotational, and γ -soft nuclei, respectively [2, 3]. However, many researchers have suggested that nuclei may have an intermediate structure consisting of the transitions $U(5)$ - $SU(3)$, $U(5)$ - $O(6)$, and $SU(3)$ - $O(6)$ [4, 5].

Great deal of research on the structure of electromagnetic transitions and energy levels in even-even Cd isotopes have been carried out [6–12]. The stable isotopes of $^{110,112}\text{Cd}$ have already been explained as collective nuclei with multiphonon excitations. Morrison and Smith [13] presented four distinct constant boson interactions in order to illustrate the framework of $^{108,116}\text{Cd}$ isotopes for states with angular momentum ($L=1$ to 6). Pignanelli *et al.* [14] used the interacting boson model to study the octupole excitations in nuclei with masses between 98 and 150. The low-spin state in even-even $^{106-112,116}\text{Cd}$ isotopes was examined utilizing γ -ray (in/off-beam) and conversion-electron spectroscopy [15]. Long *et al.* [7] used IBM-1 to explain the low-lying levels and high-spin states of $^{116,118,120}\text{Cd}$. The same

procedure was also carried out by Bollaert *et al.* [16]. Moreover, Kadi *et al.* [17] used the (n,n',γ) reaction to investigate the lifetimes of various levels as well as the decay parameters of multiphonon quadrupole vibrational states and invasion structures in ^{116}Cd . They found that the intruder pattern is fully confirmed in the ^{116}Cd nuclei. Likewise, Gade *et al.* [18] evaluated the electric and magnetic dipole excitations of ^{108}Cd nuclei and estimated the lifetimes of eight dipoles. Furthermore, the researchers demonstrated a transition path between the dynamic $U(5)$ and $O(6)$ limits for the ^{108}Cd using the IBM-2 framework. Garrett *et al.* [19] used the interaction boson model to analyze the systematic variation of $^{110-114}\text{Cd}$ isotopes. Their calculations show that Cd isotopes at the two-photon levels reflect the data quite well, while the calculations for the 0^+ states in ^{116}Cd fail completely. Systematic variations occur across the Cd isotopic chain at the three-phonon level, demonstrating the breakdown of vibrational motion in low-spin states. Hossian *et al.* [20] used IBM-1 to study the energy level of $^{104-122}\text{Cd}$ nuclides. They noted that Cd isotopes have a vibrational symmetry $U(5)$. The resulting Hamiltonian was utilized by Nomura *et al.* [21] to calculate the low-lying excitation bands, quadrupole and monopole electrical transition rates for the even-even $^{108-116}\text{Cd}$. Many intruder states were predicted, which corresponded to empirical data. Besides, Leviatan *et al.* [22] show that vibrational symmetry is retained in a part of the ^{110}Cd spectrum and destroyed in certain nonyrast states. In addition, the vibration in the bulk of the low-lying normal states is reportedly preserved. Besides the IBM-1, Harris [23] and Mariscotti *et al.* [24] for example, used a framework in which higher-order nuclear angular velocity terms in the cranking model were preserved as well as the moment of inertia was extended to excited bands with two variables (g_o and C). Raduta *et al.* [25] de-quantized a second-order quadrupole boson using a time-dependent vari-

ation principle. They applied the coherent state model technique on nuclei, and used the least squares method to calculate the implicated parameters. This paper aims to use the interacting boson model (IBM-1) with a new empirical equation (NEE) to calculate the ground and other states for even-even ^{114–128}Cd isotopes. The EPS contour was examined for Cd nuclei. In addition, the reduced transition probabilities B(E2) are determined and compared to experimental data.

2. Calculation procedure

For nuclei containing N nucleons, the Interacting Boson Model (IBM) assigns the occupancy to a truncated model space. It provides a quantitative interpretation of indistinguishable particles with angular momentum equal to either 0 or 2 forming pairs. In IBM-1, the Hamiltonian is written as [6, 26]

$$\begin{aligned}
H = & \varepsilon_s(s^\dagger \cdot \tilde{s}) + \varepsilon_d(d^\dagger \cdot \tilde{d}) + \sum_{L=0,2,4} \frac{1}{2}(2L+1)^{1/2} C_L \left[[d^\dagger \times d^\dagger] \times [\tilde{d} \times \tilde{d}] \right]^{(0)} + \frac{1}{\sqrt{2}} \nu_2 \left[[d^\dagger \times d^\dagger]^{(2)} \times [\tilde{d} \times \tilde{s}]^{(2)} \right. \\
& \left. + [d^\dagger \times s^\dagger]^{(2)} \times [\tilde{d} \times \tilde{d}]^{(2)} \right]^{(0)} + \frac{1}{2} \nu_o \left[[d^\dagger \times d^\dagger]^{(0)} \times [\tilde{s} \times \tilde{s}]^{(0)} + [s^\dagger \times s^\dagger]^{(0)} \times [\tilde{d} \times \tilde{d}]^{(0)} \right]^{(0)} \\
& + \frac{1}{2} u_o \left[[s^\dagger \times s^\dagger]^{(0)} \times [\tilde{s} \times \tilde{s}]^{(0)} + u_2 \left[[d^\dagger \times s^\dagger]^{(2)} \times [\tilde{d} \times \tilde{s}]^{(2)} \right]^{(0)} \right]. \tag{1}
\end{aligned}$$

The IBM-1 Hamiltonian can be described in nine terms, two of which appear in one-body terms (s and d). The ε_s and ε_d denote the energy of bosons, while the rest are two-body terms ($C_0, C_1, C_4, \nu_0, \nu_2, u_0, u_2$). The number of bosons N_b , on the other hand, is conserved. In general, the IBM-1 Hamiltonian in Eq. (1) can also be expressed as [28]

$$\hat{H} = \varepsilon \hat{n}_d + a_o \hat{P} \cdot \hat{P} + a_1 \hat{L} \cdot \hat{L} + a_2 \hat{Q} \cdot \hat{Q} + a_3 \hat{T}_3 \cdot \hat{T}_3 + a_4 \hat{P}_4 \cdot \hat{T}_4, \tag{2}$$

where $\varepsilon = \varepsilon_d - \varepsilon_s$ is the boson energy, and the operators are defined as follows:

$$\begin{aligned}
\hat{n}_d = & d^\dagger \cdot \tilde{d}, \quad \hat{P} = \frac{1}{2} [(\tilde{d} \cdot \tilde{d}) - (\tilde{s} \cdot \tilde{s})], \quad \hat{L} = \sqrt{10} [d^\dagger \times \tilde{d}]^{(1)}, \\
\hat{Q} = & [d^\dagger \times \tilde{s} + s^\dagger \times \tilde{d}] + \chi [d^\dagger \times \tilde{d}]^{(2)}, \quad \hat{T}_r = [d^\dagger \times \tilde{d}]^{(r)}. \tag{3}
\end{aligned}$$

Total number of d-bosons, pairing, angular momentum, and quadrupole are represented by the operators $\hat{n}_d, \hat{P}, \hat{L}, \hat{Q}$ respectively. The \hat{T}_r operator represents to octupole and hexadecapole as $r = 3$ and 4, respectively, and H refers to the quadrupole structure parameter. The strength parameters $a_0, a_1, a_2, a_3,$ and a_4 are used to describe the interactions between the bosons. The operator \tilde{d} is equal to $(-1)^m d_{-m}$. Interaction parameters for the PHINT program are specified: ε =EPS, a_0 =PAIR, a_1 =ELL/2, a_2 =QQ/2, a_3 =5 OCT, a_4 +5 HEX, and CHI=0.

The IBM-1 performs three types of dynamic symmetry for nuclei: vibrational U(5), rotational SU(3) and γ -soft O(6), with their eigenvalues given by [28].

$$\begin{aligned}
E = & \varepsilon n_d + \beta n_d(n_d + 4) + 2\gamma\nu(\nu + 3) + 2\delta L(L + 1) \dots U(5), \\
E = & \frac{a_2}{2} (\lambda^2 + \mu^2 + \lambda\mu + 3(\lambda + \mu)) + \left(a_1 - \frac{3a_2}{8} \right) L(L + 1) \dots SU(3), \\
E = & \frac{a_o}{4} (N - \sigma)(N + \sigma + 4) + \frac{a_3}{2} \tau(\tau + 3) + \left(a_1 - \frac{a_3}{10} \right) L(L + 1) \dots O(6), \tag{4}
\end{aligned}$$

hence, the energy ε , pairing a_0 , and quadrupole a_2 parameters are influence in the U(5), O(6), and SU(3) limits, respectively. Several nuclei have a property that allows them to transition between two or three of the above-mentioned limits. The new empirical equation (NEE) [29] was used in this study to calculate the energy levels of Cd isotopes. The energy levels of the GSB are determined depending only on the angular momentum (I) as follows:

$$E(I) = \frac{A_1 I(I + 1)}{A_2(I + 1) + IA_3}. \tag{5}$$

This formula has three parameters, A_1, A_2 and A_3 . These parameters were obtained after fitting all of the positive experimental (GSB) data. Further to that, the following formula can be used to compute the other bands [29]

$$E(I) = E_o + \frac{(A_1 + B)(I(I + 1))}{A_2(I + 1) + IA_3}. \tag{6}$$

In addition, the E_0 ($I=0$) and B can be estimated from the γ -and β -bands.

TABLE I. The energy ratios of Cd isotopes.

Isotopes	^{114}Cd	^{116}Cd	^{118}Cd	^{120}Cd	^{122}Cd	^{124}Cd	^{126}Cd	^{128}Cd
$R_{4/2}$	2.29	2.38	2.39	2.38	2.33	2.26	2.25	2.21

TABLE II. Shows the IBM-1 and NEE parameters in MeV for $^{114-128}\text{Cd}$, except for N_b , A2 and A3. The pairing, angular momentum, and octupole operators are denoted by the letters PAIR, ELL, and OCT, respectively.

Isotope	N_b	IBM				NEE		
		EPS	PAIR	ELL	QQ	A_1	A_1	A_3
^{114}Cd	9	0.510	0.057	0.014	0.056	0.0018	0.0055	-8.6383
^{116}Cd	8	0	0.071	0.013	0.051	0.5147	1.6424	-2.0039
^{118}Cd	7	0	0.080	0.009	0.053	0.0335	0.1086	-3.4837
^{120}Cd	6	0	0.099	0.010	0.055	0.0760	0.2287	-2.1158
^{122}Cd	5	0.530	0.142	0.013	0.058	0.1274	0.3536	-1.64348
^{124}Cd	4	0.580	0.153	0.014	0.063	0.0001	0.0004	-12.7729
^{126}Cd	3	0.610	0.183	0.005	0.063	1.3200	3.8510	-2.6660
^{128}Cd	2	0.620	0.197	0.003	0.065	1.3179	3.8221	-2.5590

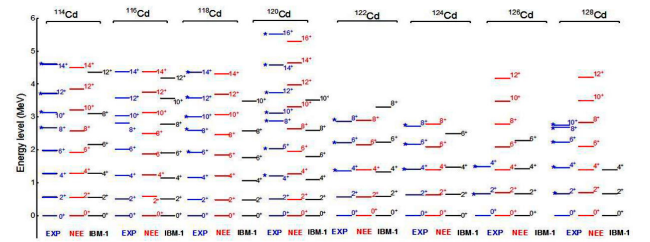
TABLE III. NEE parameters of the other band in MeV for the Cd isotopes.

Isotopes	E_o	B
^{114}Cd	1.021	-0.0005
^{116}Cd	1.1308	-0.1487
^{118}Cd	1.2231	-0.0033
^{120}Cd	1.2503	0.0005
^{122}Cd	1.4798	0.0003
^{124}Cd	1.5895	-0.2466
^{126}Cd	1.1373	0.0109
^{128}Cd	1.1700	-0.0115

3. Results and discussion

The results for the energy levels of the ground and other states for $^{114-128}\text{Cd}$ isotopes, the energy ratios $E_{4_1^+}/E_{2_1^+}$, the reduced transition probabilities $B(E2)$ results, as well as the $B(E2;4_1^+ \rightarrow 2_1^+)/B(E2;2_1^+ \rightarrow 0_1^+)$ ratios, and the potential energy surface (EPS), are discussed comprehensively below.

The simplest way to determine the IBM-1 parameters is to use the energy ratio (R) as a starting point for calculations. The energy ratio, $R=(E_{4_1^+})/(E_{2_1^+})$, indicates the symmetrical form of a nucleus. The $E_{4_1^+}$ and $E_{2_1^+}$ patterns correspond to the 4_1^+ and 2_1^+ energy levels, respectively. It is well understood that $R \approx 3.33$ stands for deformed nuclei $SU(3)$, $R \approx 2.5$ is for γ -unstable nuclei $O(6)$, and $R \approx 2$ is for vibrational nuclei $U(5)$ [30–32]. The experimental values of the energy ratio of the Cd isotopes are shown in Table I. The best values for the parameters that provide a suitable fit between the theoretical and experimental energy levels of the Cd isotopes

FIGURE 1. Experimental low-lying energies obtained from [33] in $^{114-128}\text{Cd}$ isotopes compared to IBM-1 and NEE calculations.

are shown in Table II, while Table III shows the best-fit parameters for the other bands of NEE (6).

The results of the IBM-1 and NEE calculations of the energy levels for ground and other states of the Cd isotope are presented in Figs. 1 and 2, respectively. The low-lying spectrum in Cd nuclei values of the IBM-1 and NEE are really equivalent to available experimental results for 0^+ , 2^+ , 4^+ , and 6^+ states. For the high states, the NEE and IBM-1 calculations are slightly overpredicted with the exception of the ^{114}Cd and ^{118}Cd nuclei, as illustrated in Fig. 1. The levels marked with an asterisk (*) represent cases that the spin or parity of the respective states has not been established experimentally. The IBM-1, NEE, and experimental data on the energy level structures of Cd nuclei appear at first glance to be similar for the other states, as shown in Fig. 2. However, we can render a few predictions based on a comparison of theoretical predictions and experimental results. For the IBM-1 description, the spacing between both 2^+ states is slightly overestimated in ^{114}Cd and underestimated in $^{116-118}\text{Cd}$. There is no gap between both 2^+ states in $^{114-122}\text{Cd}$ in the NEE description. Conversely, the comparison between the energies of the states, *i.e.* for the 6^+ states, is significantly improved.

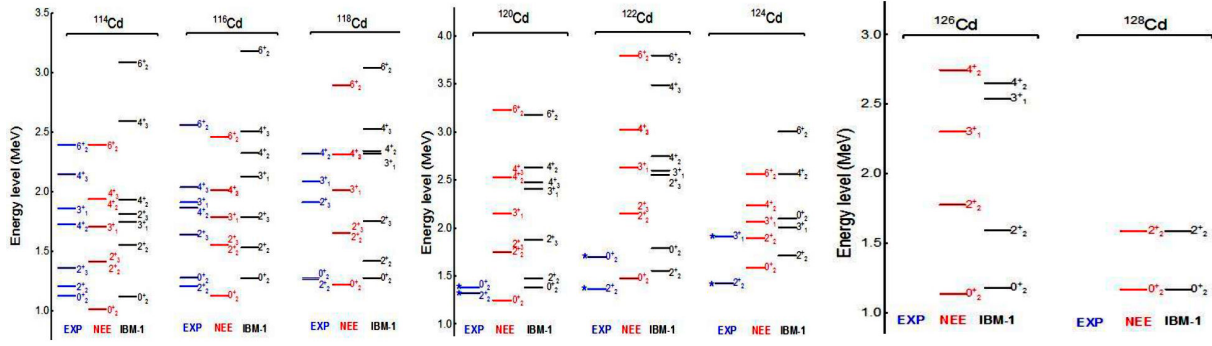


FIGURE 2. The other states of the even-even $^{114-128}\text{Cd}$ isotopes.

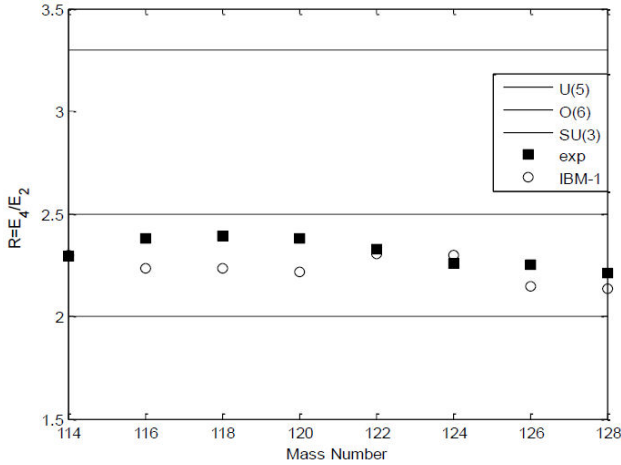


FIGURE 3. Comparison of the $(E4_1^+)/(E2_1^+)$ values for the experimental data and IBM-1 calculations with the U(5), O(6), and SU(3) limits for Cd isotopes.

As already mentioned, the symmetry shape of a nucleus can be predicted from the energy ratio $R=(E4_1^+)/(E2_1^+)$. Then, the collective dynamics of even-even nuclei energy can be classified into three subgroups: SU(3), O(6), and U(5). The $R_{4/2}$ values of low-lying energy levels of Cd isotopes vary as a function of mass number for experimental values, IBM-I, SU(3), O(6), and U(5) limits as presented in Fig. 3. The calculated energy ratios, $R_{4/2}$, of Cd nuclei agree well with experimental results, with small exceptions for $^{116-120}\text{Cd}$ nuclei. Furthermore, this figure clearly demonstrates the transition between the collective structures of U(5) and O(6). We clearly notice that the energy ratio increases very slowly with increasing the neutron number up to ^{120}Cd , after which it decreases in the experimental results. However, the IBM-1 results show relatively small fluctuations.

The electromagnetic transitions operator in IBM-1 has a general form [7, 28]:

$$\hat{T}^{(L)} = \gamma_0 [s^\dagger \times \tilde{s}]^{(0)} + \alpha_2 [d^\dagger \times \tilde{s} + s^\dagger \times \tilde{d}]^{(2)} + \beta_L [d^\dagger \times \tilde{d}]^{(L)}, \quad (7)$$

where γ_0 , α_2 , and β_L ($L=0, 1, 2, 3, 4$) are parameters identifying the different terms in the corresponding operators. The reduced electrical transition probabilities provide information about nuclei structure. The E2 transition operator is

recognized to be a Hermitian tensor. As a result, the N_b is always conserved. Then, the E2 transition operator is represented as [34]:

$$\hat{T}^{(E)} = \alpha_2 [d^\dagger s + s^\dagger d]^{(2)} + \beta_L [d^\dagger d]^{(2)}, \quad (8)$$

here, the (s^\dagger, d^\dagger) and (s, d) symbols refer to creation and annihilation operators, respectively. The α_2 represents to the effective charge for boson and β_2 is a dimensionless coefficient, $\beta_2 = \chi \alpha_2$. The $B(E2)$ values for electrical transition probabilities are described in terms of reduced matrix elements as [28, 34, 35]:

$$B\left((E_2)I_i \rightarrow I_f\right) = \frac{1}{2L_i + 1} |\langle I_f || T^{(E_2)} || I_i \rangle|^2. \quad (9)$$

The effective charges e_B for Cd isotopes are shown in Table IV. The experimental values of $B(E2)$: $2_1^+ \rightarrow 0_1^+$ were reproduced from the e_B values. The results of the IBM-1 and available experimental data for $B(E2)$ values of ($g \rightarrow g$, $\beta \rightarrow \beta$, $\gamma \rightarrow \gamma$ and $\gamma \rightarrow \beta$) transitions for $^{114-128}\text{Cd}$ isotopes are shown in Table V. Furthermore, the results of the ground state bands of $B(E2)$ data for ($2_1^+ \rightarrow 0_1^+$, $4_1^+ \rightarrow 2_1^+$, $6_1^+ \rightarrow 4_1^+$, $8_1^+ \rightarrow 6_1^+$) levels demonstrated that the IBM-1 calculations with the experimental data for $^{114-120}\text{Cd}$ isotopes matched with the maximum associated error of 23%, while experimental data are lacking for the other Cd isotopes. The $B(E2, 2_1^+ \rightarrow 0_1^+)$ of $^{114-118}\text{Cd}$ isotopes gradually increases as the number of neutrons increases. For the other

TABLE IV. $B(E2)$ values for $^{114-128}\text{Cd}$ were reproduced using an effective charge, e_B .

Isotope	N_b	e_B (eb)
^{114}Cd	9	0.071
^{116}Cd	8	0.076
^{118}Cd	7	0.085
^{120}Cd	6	0.087
^{122}Cd	5	0.093
^{124}Cd	4	0.098
^{126}Cd	3	0.104
^{128}Hf	2	0.109

TABLE V. Theoretical versus experimental $B(E2)$ for $^{114-128}\text{Cd}$ isotopes in unit of e^2b^2 are compared.

$I_i \rightarrow I_f$	^{114}Cd		^{116}Cd		^{118}Cd	
	EXP.	IBM-1	EXP.	IBM-1	EXP.	IBM-1
$2_1^+ \rightarrow 0_1^+$	0.102	0.101	0.113	0.112	0.114	0.114
$2_3^+ \rightarrow 0_2^+$	0.213	0.267	—	0.070	—	0.065
$2_2^+ \rightarrow 2_1^+$	0.072	0.141	0.084	0.152	—	0.148
$2_3^+ \rightarrow 2_2^+$	0.089	0.043	—	0.000	—	0.000
$2_3^+ \rightarrow 4_1^+$	0.148	0.090	—	0.000	—	0.000
$4_1^+ \rightarrow 2_1^+$	0.203	0.152	0.188	0.152	0.209	0.184
$4_2^+ \rightarrow 2_2^+$	0.105	0.083	—	0.000	—	0.082
$4_2^+ \rightarrow 2_3^+$	0.390	0.152	—	0.092	—	0.000
$4_2^+ \rightarrow 4_1^+$	0.058	0.075	0.504	0.342	—	0.074
$6_1^+ \rightarrow 4_1^+$	0.390	0.258	0.361	0.2961	—	0.156
$6_2^+ \rightarrow 4_2^+$	0.426	0.261	—	0.094	—	0.000
$8_1^+ \rightarrow 6_1^+$	0.283	0.161	—	0.159	—	0.147
	^{120}Cd		^{122}Cd		^{124}Cd	
$I_i \rightarrow I_f$	EXP.	IBM-1	EXP.	IBM-1	EXP.	IBM-1
$2_1^+ \rightarrow 0_1^+$	—	0.091	0.093	0.089	—	0.059
$2_2^+ \rightarrow 2_1^+$	—	0.118	—	0.115	—	—
$4_1^+ \rightarrow 2_1^+$	—	0.118	—	0.115	—	0.072
$4_2^+ \rightarrow 2_2^+$	—	0.063	—	0.058	—	—
$4_2^+ \rightarrow 4_1^+$	—	0.058	—	0.112	—	—
$6_1^+ \rightarrow 4_1^+$	—	0.121	—	0.089	—	0.063
$8_1^+ \rightarrow 6_1^+$	—	0.107	—	0.089	—	0.038
	^{126}Cd		^{128}Cd			
$I_i \rightarrow I_f$	EXP.	IBM-1	EXP.	IBM-1		
$2_1^+ \rightarrow 0_1^+$	—	0.069	—	0.072		
$2_2^+ \rightarrow 2_1^+$	—	0.083	—	0.072		
$4_1^+ \rightarrow 2_1^+$	—	0.083	—	0.072		
$4_2^+ \rightarrow 2_2^+$	—	0.031	—	—		
$4_2^+ \rightarrow 4_1^+$	—	0.028	—	—		
$6_1^+ \rightarrow 4_1^+$	—	0.059	—	—		

isotopes, however, the $B(E2)$ values tend to fluctuate, confirming that these states are expected to be deformed. Moreover, the $B(E2; 2_2^+ \rightarrow 2_1^+)$ decreases with increasing neutron number, except for ^{114}Cd isotope. Other transitional levels exhibit similar variations and can be interpreted similarly. The experimentally published and determined $B(E2)$ values for $^{114-128}\text{Cd}$ isotopes generally agree well in some places. Other important quantities, such as the $B(E2)$ ratio, are used to demonstrate that the Cd isotopes are deformed nuclei and tend to have a dynamical symmetry $U(5)$ - $O(6)$. For all nuclei under inquiry, the $B(E2)$ ratio is calculated and presented in Fig. 4. The comparison of experimental data and IBM-1 calculations for Cd isotopes is also shown in this figure. We also calculated the $B(E2; 4_1^+ \rightarrow 2_1^+)/B(E2; 2_1^+ \rightarrow 0_1^+)$ ratio in Cd isotopes, and found that the $B(E2)$ ratio shows almost little variations

with respect to the isotope mass number. These values are smaller than the corresponding γ -unstable nuclei $O(6)$ and approach the vibrational limit $U(5)$. Moreover, the theoretical values of the $B(E2)$ ratio for these nuclei are in good agreement with the experimental data. As a result, Cd isotopes are closer to the $U(5)$ - $O(6)$ boundary.

The potential energy surface (EPS) application provides information to determine the microscopic and geometric shapes of nuclei. IBM Hamiltonian produced the EPS plots using the Skyrme mean field procedure [30]. The IBM-1 energy surface is constructed by combining the IBM-1 Hamiltonian's expectation value with the coherent state $(|N, B, \gamma\rangle)$ [6]. The creation operators (b_i^\dagger) act on a state of boson vacuum $|0\rangle$ to produce the coherent state as follows [31, 36]:

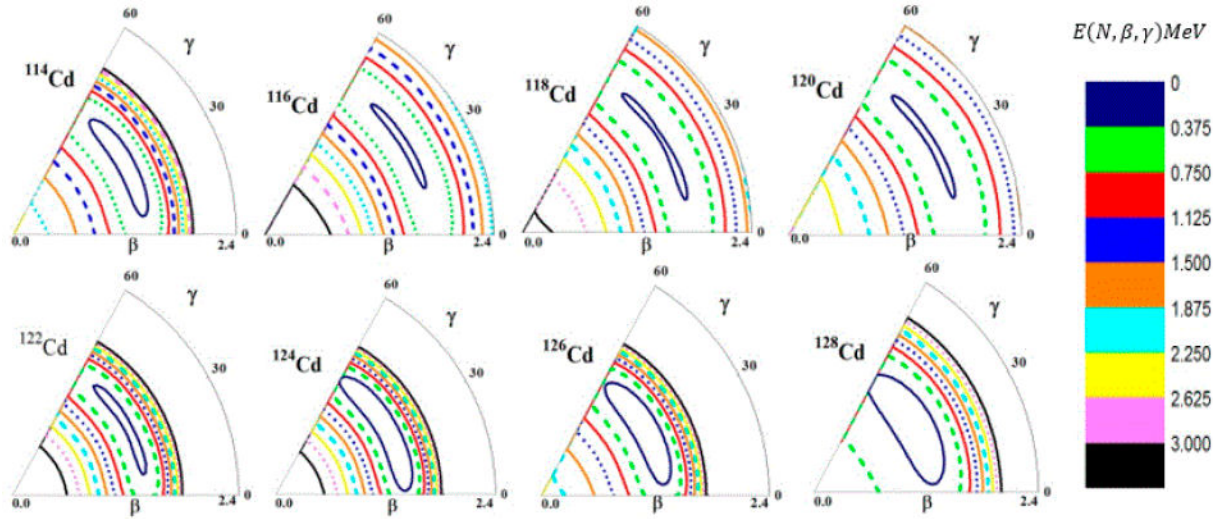


FIGURE 5. The EPS contour plot for $^{114-128}\text{Cd}$ nuclei. The color panel represents the EPS values in MeV.

$$|N, B, \gamma \rangle = 1/\sqrt{N!}(b_c^\dagger)^N |0 \rangle, \quad (10)$$

where

$$b_c^\dagger = (1 + \beta^2)^{1/2} \times \left\{ \beta \left[\cos \gamma (d_0^\dagger) + \sqrt{1/2} \sin \gamma (d_2^\dagger + d_{-2}^\dagger) \right] \right\}, \quad (11)$$

then, the EPS can be written in terms of β and γ as [32]:

$$E(N, \beta, \gamma) = \frac{N\varepsilon_d\beta^2}{(1 + \beta^2)} + \frac{N(N + 1)}{(1 + \beta^2)^2} \times (\alpha_1\beta^2 + \alpha_2\beta^3 \cos 3\gamma + \alpha_3\beta^2 + \alpha_4). \quad (12)$$

Where α' s parameters are associated with the coefficient of C_L , v_2 , v_o , and u_o , as seen in Eq. (1). The term β refers to a nucleus total deformation. Then, the shape of a nucleus could be spherical or distorted depending on whether $\beta = 0$ or not. Moreover, the variation in nucleus symmetry is represented by γ term, when $\gamma = 0$, the nucleus has a prolate shape; when $\gamma = 60$, it has an oblate shape. The deformation energy surfaces of the even-even isotopes $^{114-128}\text{Cd}$ were estimated as plotted in Fig. 5. The energy surfaces formed a prolate and a slightly oblate threshold that should correlate with proton normal and intruder excitations [21]. The $^{116-120}\text{Cd}$ nuclei, on the other hand, have a deformation shape and a γ -unstable character ($\gamma \approx 30$). While the isotopes $^{114,122,124,126,128}\text{Cd}$ have a potential energy surface that is

approximately independent of the triaxial γ -parameter. The U(5)-O(6) transitions were identified in the EPS map for Cd nuclei in the (β, γ) deformation space.

4. Conclusions

Using the IBM-1 and NEE methods, the ground and other state energies, the electromagnetic transition, and the potential energy surface of $^{114-128}\text{Cd}$ isotopes were all calculated theoretically. The results of the ground and other energy levels of Cd isotopes are consistent in some places with previous experimental data, *i.e.*, the description of the energies of the 2^+ state is not well represented in the IBM-1 model. Furthermore, the results of the IBM-1 on reduced transition probabilities B(E2) roughly agree with the available experimental data. Similarly, the $B(E2; 4_1^+ \rightarrow 2_1^+)/B(E2; 2_1^+ \rightarrow 0_1^+)$ ratio in Cd isotopes varies relatively minimally with respect to nuclear mass number. The EPS contour results for Cd isotopes demonstrate that the investigated Cd isotopes represent a shape phase change from vibrational U(5) to γ -soft O(6) dynamical symmetry. Finally, the $^{114-128}\text{Cd}$ nuclei are minimally prolate and exhibit moderate axial distortion.

Acknowledgements

We are grateful to the University of Mosul, College of Education for Pure Sciences, Department of Physics for their assistance with this research work.

1. H. Lehmann, and Garrett, PE and Jolie, J and McGrath, CA and Yeh, Minfang and Yates, SW, On the nature of three-phonon excitations in ^{112}Cd , *Physics Letters B* **387** (1996) 259-26, <https://doi.org/10.1016/>

0370-2693(96)01038-6

2. F. Corminboeuf *et al.*, Structures and lifetimes of states in ^{110}Cd . *Physical Review C* **63** (2000) 014305, <https://doi.org/>

- org/10.1103/PhysRevC.63.014305
3. P. J. Davies *et al.*, The role of core excitations in the structure and decay of the 16^+ spin-gap isomer in ^{96}Cd . *Physics Letters B* **767** (2017) 474-479, <https://doi.org/10.1016/j.physletb.2017.02.013>
 4. G. Lorusso *et al.*, β -decay half-lives of 110 neutron-rich nuclei across the $N=82$ shell gap: implications for the mechanism and universality of the astrophysical r process. *Physical review letters* **114** (2015) 192501, <https://doi.org/10.1103/PhysRevLett.114.192501>
 5. Scharff-Goldhaber, Gertrude, and J. Weneser, System of even-even nuclei. *Physical Review* **98** (1955) 212, <https://doi.org/10.1103/PhysRev.98.212>
 6. F. Iachello and A. Arima, The interacting boson model Cambridge Uni. Press, Cambridge (1987).
 7. G. L. Long, S. J. Zhu and H. Z. Sun, Description of $^{116,118,120}\text{Cd}$ in the interacting boson model, *Journal of Physics G: Nuclear and Particle Physics* **21** (1995) 331, <https://doi.org/10.1088/0954-3899/21/3/008>
 8. F. Iachello, Analytic description of critical point nuclei in a spherical-axially deformed shape phase transition. *Phys. Rev. Lett.* **87** (2001) 052502, <https://doi.org/10.1103/PhysRevLett.87.052502>
 9. A. K. Mheemmed, A. Kh Hussein, and R. B. Kheder, Characterization of alpha-particle tracks in cellulose nitrate LR-115 detectors at various incident energies and angles. *Applied Radiation and isotopes* **79** (2013) 48, <https://doi.org/10.1016/j.apradiso.2013.04.020>
 10. P. Cejnar, Jan Jolie, and R. F. Casten, Quantum phase transitions in the shapes of atomic nuclei. *Reviews of Modern Physics* **82** (2010) 2155, <https://doi.org/10.1103/RevModPhys.82.2155>
 11. H. H. Kassim, A. A. Abd-Aljbar, M. Abed Al-Jubbori, H. Y. Abdullah, I. Hossain, and F. I. Sharrad, Properties of $O(6)-U(5)$ transition symmetry for $^{122-124}\text{Cd}$ isotopes in IBM. *In IOP Conference Series: Materials Science and Engineering*, **928** (2020) 072149. <https://doi.org/10.1088/1757-899X/928/7/072149>
 12. I. Hossain, H. Y. Abdullah, I. M. Ahmed, and M. A. Saeed, Ground-state energy band of even $^{104-122}\text{Cd}$ isotopes under the framework of interacting boson model-1: a review. *Journal of Theoretical and Applied Physics* **7** (2013) 1-5, <https://doi.org/10.1186/2251-7235-7-46>
 13. I. Morrison, and R. Smith, The interacting boson approximation and the spectroscopy of the even cadmium and tin isotopes. *Nuclear Physics A* **350** (1980) 89-108, [https://doi.org/10.1016/0375-9474\(80\)90390-5](https://doi.org/10.1016/0375-9474(80)90390-5)
 14. M. Pignanelli *et al.*, Octupole excitations in vibrational nuclei and the sdf interacting boson model. *Nuclear Physics A* **519** (1990) 567-601, [https://doi.org/10.1016/0375-9474\(90\)90447-T](https://doi.org/10.1016/0375-9474(90)90447-T)
 15. J. Kumpulainen *et al.*, Systematic study of low-spin states in even Cd nuclei. *Physical Review C* **45** (1992) 640, <https://doi.org/10.1103/PhysRevC.45.640>
 16. N. Boelaert, N. Smirnova, K. Heyde, and J. Jolie, Shell model description of the low-lying states of the neutron deficient Cd isotopes. *Phys. Rev. C* **75** (2007) 014316, <https://doi.org/10.1103/PhysRevC.75.014316>
 17. M. Kadi, N. Warr, P. E. Garrett, J. Jolie, and S. W. Yates, Vibrational and intruder structures in ^{116}Cd . *Phys. Rev. C* **68** (2003) 031306, <https://doi.org/10.1103/PhysRevC.68.031306>
 18. A. Gade *et al.*, Dipole excitations in ^{108}Cd . *Phys. Rev. C* **67** (2003) 03430, <https://doi.org/10.1103/PhysRevC.67.034304>
 19. Garrett, PE and Green, KL and Wood, JL, Breakdown of vibrational motion in the isotopes Cd $^{110-116}$, *Phys. Rev. C*, **78** (2008) 044307, <https://doi.org/10.1103/PhysRevC.78.044307>
 20. Hossain, I., Hewa Y. Abdullah, I. M. Ahmed, M. A. Saeed, and S. T. Ahmad. Study on ground state energy band of even $^{114-124}\text{Cd}$ isotopes under the framework of interacting boson model (IBM-1). *International J. Modern Phys. E* **21** (2012) 1250072, <https://doi.org/10.1142/S0218301312500723>
 21. K. Nomura, and J. Jolie, Structure of even-even cadmium isotopes from the beyond-mean-field interacting boson model. *Phys. Rev. C* **98** (2018) 024303, <https://doi.org/10.1103/PhysRevC.98.024303>
 22. A. Leviatan, and N. Gavrielov, J. E. García-Ramos, and P. Van Isacker, Quadrupole phonons in the cadmium isotopes. *Physical Review C* **98** (2018) 031302, <https://doi.org/10.1103/PhysRevC.98.031302>
 23. S. M. Harris, Higher order corrections to the cranking model. *Physical Review* **138** (1965) B509. <https://doi.org/10.1103/PhysRev.138.B509>
 24. Mo Ao J. Mariscotti, Gertrude Scharff-Goldhaber, and Brian Buck. Phenomenological analysis of ground-state bands in even-even nuclei. *Phys. Rev.* **178** (1969), 1864, <https://doi.org/10.1103/PhysRev.178.1864>
 25. A. A. Raduta, R. Budaca, and A. Faessler, Analytical description of the coherent state model for near vibrational and well deformed nuclei. *Annals of Physics* **327** (2012) 671-704, <https://doi.org/10.1016/j.aop.2011.10.004>
 26. A. Arima, and F. Iachello, Interacting boson model of collective states I. The vibrational limit. *Annals of Phys.* **281** (2000) 2-64, <https://doi.org/10.1006/aphy.2000.6007>
 27. R. C. Ewing, W. J. Weber, and F. W. Clinard Jr., Radiation effects in nuclear waste forms for high-level radioactive waste. *Progress in nuclear energy* **29** (1995) 63-127, [https://doi.org/10.1016/0149-1970\(94\)00016-Y](https://doi.org/10.1016/0149-1970(94)00016-Y)
 28. R. F. Casten and D. D. Warner, The interacting boson approximation. *Rev. Mod. Phys.* **60** (1988) 389, <https://doi.org/10.1103/RevModPhys.60.389>
 29. A. Jubbori, M. Abed, H. H. Kassim, F. I. Sharrad, and I. Hossain. Deformation properties of the even-even rare-earth Er-Os isotopes for $N=100$. *International Journal of Modern Physics E* **27** (2018) 1850035, <https://doi.org/10.1142/S0218301318500350>
 30. R. F. Casten, and N. V. Zamfir, Empirical realization of a critical point description in atomic nuclei. *Physical Review Letters* **87** (2001) 052503, <https://doi.org/10.1103/PhysRevLett.87.052503>

31. A.-Jubbori, M. A., Huda H. Kassim, F. I. Sharrad, and I. Hos-sain, Nuclear structure of even 120–136 Ba under the frame-work of IBM, IVBM and new method (SEF). *Nucl. phys. A.* **955** (2016) 101-115. <https://doi.org/10.1016/j.nuclphysa.2016.06.005>
32. H. H. Khudher, A. K. Hasan, and F. I. Sharrad, Calculation of energy levels, transition probabilities, and potential energy sur-faces for 120-126 Xe even-even isotopes. *Ukrainian J. Phys.* **62** (2017) 152-158,
33. <http://www.nndc.bnl.gov/chart/getENSDFDatasets.jsp>
34. H. H. Kassim, and F. I. Sharrad, Energy levels and electro-magnetic transition of 190–196 Pt nuclei. *International Journal of Modern Physics E* **23** (2014), 1450070, <https://doi.org/10.1142/S0218301314500700>
35. H. H. Kassim *et al.*, Nuclear structure of Even 178–182 Hf Iso-topes Under the Framework of Interacting Boson Model (IBM-1). *Iranian J. Science and Technology, Transactions A: Sci-ence* **42** (2018) 993-999, <https://doi.org/10.1007/s40995-016-0104-x>
36. A. E. L. Dieperink, O. Scholten, and F. Iachello, Clas-sical limit of the interacting-boson model. *Phys. Rev. Lett.* **44** (1980) 1747, <https://doi.org/10.1103/PhysRevLett.44.1747>